ELSEVIER

Journal of Chromatography A, 818 (1998) 155–168

JOURNAL OF CHROMATOGRAPHY A

Measurement of the degree of internal friction of two native silica packing materials

Kathleen Mihlbachler[a,b], Thomas Kollmann[c], Andreas Seidel-Morgenstern[c], Jürgen Tomas[c], Georges Guiochon[a,b,*]

[a]*Department of Chemistry, The University of Tennessee, Knoxville, TN 37996-1600, USA*
[b]*Division of Chemical and Analytical Sciences, Oak Ridge National Laboratory, Oak Ridge, TN 37861, USA*
[c]*Institut für Verfahrenstechnik, Otto-Von-Guericke Universität, Magdeburg, Germany*

Received 10 April 1998; received in revised form 24 June 1998; accepted 24 June 1998

Abstract

The degree of internal friction of two different packing materials for liquid chromatography (Kromasil NP10 and DuPont Pro Sil) has been measured using conventional methods of the mechanics of continuous solids applied in the study of the storage, handling and processing of powders. The former material was found to have a lower angle of internal friction and to flow more freely than the latter one. Possible relationships between these properties and the qualities of the column beds obtained are discussed.

Keywords: Silica; Packing materials; Friction

1. Introduction

In many respects, the phenomena which take place during the packing of chromatographic column beds are similar to those which occur during the filling of storage bins with powders such as flour or cement. This is especially true in the case of wide diameter columns used for preparative applications. Particles do not behave independently from each other but interact with their close neighbors, somewhat as, on a much smaller scale, molecules interact with each other in liquids. The analogy should not be taken too far, however. If there is a strong repulsion between particles in close contact, there is only a weak attraction at short distances and, potentially, an intense friction between particles in contact. This solid friction, which has no equivalent at the molecular scale, plays an important role in the behavior of bulk amounts of packing materials [1]. Because of this friction, internal stresses develop inside column beds. These stresses are transferred to the wall and a wall friction resistance is observed. However, internal stress in solids is not conveyed as pressure is in liquids. In bulk granulated materials, stress is not homogeneous [1]. Its local value depends largely on the intensity of the friction between the particles and between the bed of particles and the wall of the container, whether a chromatographic column or a storage bin. Filling up a tank with a liquid results in a pressure on the bottom of the container equal to the weight of liquid divided by the cross-section area of the vessel. This is true when piling up a granulated

*Corresponding author. Address for correspondence: Department of Chemistry, University of Tennessee, 522 Buehlir Hall, 300 South College, Knoxville, TN 37996-1600, USA.

0021-9673/98/$19.00
PII: S0021-9673(98)00546-9

material in a bin only up to heights of a few container diameters. Above that, the pressure[1] at the bottom of the bin tends toward a constant, the rest of the weight being conveyed directly as a vertical stress to the wall [1]. This phenomenon has profound consequences for the preparation and stability of column beds. It is illustrated in Fig. 1.

Thus, the performance of a chromatographic column and the modeling of a separation requires knowledge about the mechanical properties and the structure of the packing material. The various relevant mechanical properties can be determined through different procedures [2,3]. Some of the most important of these properties regard the stress distribution in the packing material contained in a chromatographic column. This paper discusses the determination of the characteristics of this stress with the help of the Jenike shear cell (JSC) [4] or of similar devices [2,3]. Shear cells are usually applied to study the consolidation effects of solids during their storage in bins or tanks and their flow in and out of these containers [5,6]. It must be emphasized, however, that the materials typically tested in the JSCs often have a larger average particle size and typically a far wider particle size distribution than the packing materials used in chromatography. Furthermore, the typical levels of compression stress encountered in the mechanics of granulated materials are usually much lower than the stress used in chromatography, whether consolidating column beds with mechanical or fluid compression. In the former case, typical stresses are between 1 and 200 kPa (~0.01 to 2 atm) and the external porosity is close to 0.5; in the latter case, typical stresses are between ten and several hundred atm and the external porosity of the bed is close to 0.4. Thus, the results obtained with the JSC require careful interpretation.

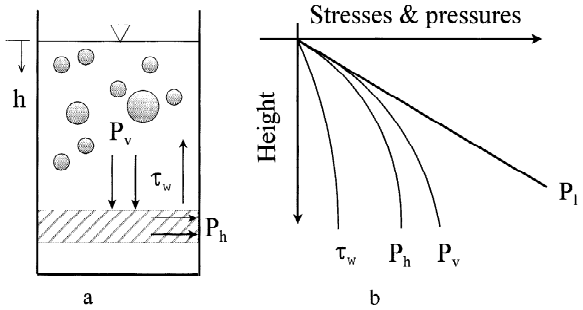

Fig. 1. Comparison between the distribution of stresses in a tank filled with a liquid and in a tall storage bin filled with a powder. (a) Cut through the container and definitions. (b) Plots of the stresses or pressures versus the height in the container. P_l, hydrostatic pressure; P_h, P_v, horizontal and vertical pressures in the heap of particles; τ_w, wall shear stress or wall friction. The ratio $\lambda = P_h/P_v$ or horizontal pressure ratio is equal to 1 in liquids and to 0 in solids. In powders, $\lambda = f(\varphi_i)$ is between 0 and 1. This shows the importance of the angle of internal friction, φ_i.

[1]In the mechanics of particulate solids, the compression stress is often called pressure. We conform to this tradition in this paper. The reader should remember that pressure (i.e., compression stress) behaves quite differently in solids and liquids.

Thus, the properties of granulated materials are important in chromatography, in connection with the preparation of efficient columns and with their long-term stability. We are concerned here with the behavior of large numbers of particles densely packed in a container (there are approximately two billions of 10-μm particles of porous silica per gram of packing material, packed with an external porosity between 0.38 and 0.43). More specifically, we are interested in their solid and liquid flow behavior and in the interactions between the bed of packing materials and the column wall. This requires the use of concepts and methods borrowed from the mechanics of granulated materials [1–13].

The aim of this paper is to present a brief outline of the concepts of the mechanics of solid particles that are relevant to the packing of column beds, to report on the results of the testing of a few typical packing materials with the JSC, and to illustrate the consequences which can be derived from this type of study. However, this work will not propose any new approaches to the modeling of the stress behavior of packing materials in chromatographic columns nor will it give any theoretical explanations of the observed behavior of the materials used.

2. Theory

The study of the behavior of granulated materials is a chapter of soil mechanics [7,9,11,13], itself a part of solid mechanics. Its essential conclusion is that large amounts of solid particles behave either as most unusual solids or most unusual liquids, depending on the experimental conditions [1]. Any analogy

that one may attempt to draw between the behavior of a bed of stationary phase particles and that of a solid body or of a liquid in a container is bound to fail. The essential reason for the latter type of comparisons is the negligibly small value of the thermal energy term, k_T, for a particle, compared with its potential energy [1]. The thermal energy at ambient temperature of a single 10-μm silica particle ($4 \cdot 10^{-21}$ J) is two orders of magnitude smaller than the increase of its potential energy in the gravity field associated with elevating its mass center by 1% of its diameter ($5 \cdot 10^{-19}$ J). As a consequence, there is no entropy term and most phenomena will be controlled by the particle dynamics in the system considered. Other differences with molecular behavior come from the facts that collisions are inelastic, that a significant fraction of the kinetic energy in a collision is turned into heat, and that there is friction between particles [1]. Typical, relevant examples of the differences between the behavior of granular and conventional materials are given now.

(a) A conical heap of powder is stable as long as the slope is lower than a certain threshold, the angle of repose [1]. Such an effect could never happen with a liquid. The angle of repose depends on the material, particularly on the nature and smoothness of the particle surface. Thus, a particulate solid has a certain shear strength, by contrast with a liquid, which has none.

(b) When filling a vertical bin with particles, the stress on the bottom of the container increases more slowly than the height of the bed and tends toward a limit as emphasized in the introduction [1]. There is a static angle of internal friction between particles. Under stress, granular solids consolidate and acquire cohesive strength in the process. Chains of particles bearing most of the mechanical stress have been identified in such beds, due to the birefringence caused by the local stress [1]. The mechanical stress is conveyed by these chains to the wall of the container. When the bed is high enough, the weight of the additional material is entirely conveyed to the container wall, no longer to its bottom.

(c) When in suspension, a granular material has no strength. When consolidated, it acquires some that increases with increasing compression pressure (Fig. 2lines a or b). The strength acquired by the consolidated material depends on the solid. Line a corresponds to a more free-flowing solid than line b. To force a material to flow through a device (e.g., a hopper), a certain pressure must be applied. There is a flow factor for the device (Fig. 2, dashed line). If the flow function of the solid is below the flow factor of the device (line a), the solid strength is insufficient to support a dome and the solid will flow freely. If the flow function of the solid is above the flow factor (line b), a dome is formed and there is no flow [4].

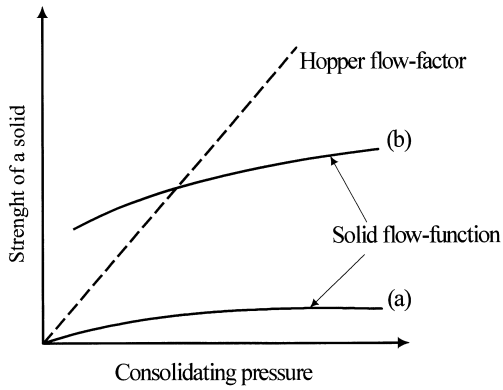

Fig. 2. Strength versus consolidation pressure [4]. Flow takes place when the solid flow function (solid line) is below the flow factor of the hopper or the storage bin (dashed line).

Because it is necessary to bridge conventional soil mechanics and the problems of concern in liquid chromatography, we consider first the flow behavior of a packing material in a hopper. We assume that this is a good model of the behavior of the dense slurry during the last stages of the consolidation of a column bed, at the end of the packing operation, when particles are in close contact with their neighbors but are not yet completely settled. There is a short step of plastic flow of the packing material which is of critical importance for the efficiency of the column.

Consider a volume element flowing along a hopper. New material is constantly added to the top, while stored material is withdrawn from the bottom. At the beginning, the pressures or compression stresses[2], σ, acting on this element increase as the element gets buried under an increasingly high

[2]Because, in a solid, compression stress is not conveyed homogeneously as pressure is in a liquid, there is a different compression stress in each direction of space.

amount of new material. At the same time, the shape of the volume element changes, it shrinks under increasing pressure, expands back when the pressure decreases, and the particles that it contains slide against each other. The interactions between individual particles integrate into local stresses. For the classical differential element of volume, (d*x*, d*y*, d*z*), there are three compression stresses, one along each axis of coordinates, and six shear stresses, two parallel to each plane of coordinates. There are relationships between the compression stress and the shear stresses acting on this volume in the three different directions of space. These relationships have been discussed and solved over 100 years ago by Cauchy and Mohr. Their detailed presentation, let alone a fundamental discussion of solid mechanics is beyond the scope of the present work. We merely summarize the relevant results and refer the interested reader to treatises on solid or soil mechanics [2,4,7,9,11,13].

A summary of the parameters needed to discuss the flowability of solids is displayed in Fig. 3 [3–6,10–13]. Note that, when the flow of granular solids is relatively slow, as it is in HPLC-related applications, the shearing stress, τ, can be considered constant and independent of the rate of shear. However, it depends on the mean pressure acting within the solid [4]. This situation is just the opposite of the one which takes place with liquid flows (the shearing stress in liquids is independent of the local pressure but depends on the rate of shear).

We simplify the problem by discussing a particular

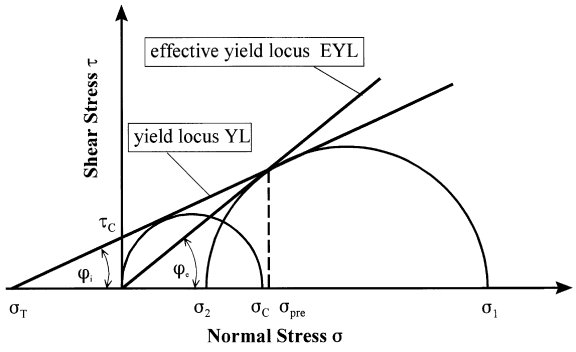

Fig. 3. Flow parameters for the yielding of bulk materials [3]. Two Mohr circles corresponding to a given powder preconsolidated under different stresses are shown.

case, linear shear, in which the solid flows in a direction parallel to a plane. Stresses are negligible in the direction *z*, perpendicular to the plane. Admittedly, this is not the situation prevalent in a chromatographic column. There are ways, however, to extend the theory presented below to the three-dimensional case [6,7,9,11] but we do not need to address this issue here. Under the conditions assumed, there are only three stresses in the *x,y* plane which are applied to a surface element perpendicular to the *x,y* plane, two compression stresses, σ_x and σ_y, and a shear stress, $\tau_{x,y}$. The numerical values of these stresses vary with the orientation of the coordinate system. It is possible to show that there are two orthogonal directions of space such that $\tau_{x,y}=0$. The two corresponding compression stresses are called the major and the minor principal stresses acting on the element, σ_1 and σ_2, respectively. In most cases, at constant temperature and water content, the ratio, σ_1/σ_2, which is called the effective yield function, is constant and given by the following equation:

$$\frac{\sigma_1}{\sigma_2}=\frac{1+\sin\varphi_e}{1-\sin\varphi_e} \tag{1}$$

where φ_e is the effective angle of internal friction [4]. This angle (usually between 30 and 70°) has been found roughly to characterize the material studied. It is smaller for dry and smooth particles, e.g., dry HPLC packing material with spherical particles, and larger for coarse, rugose and wet particles (e.g., wet packing material with irregular-shaped particles). The stresses applied to an element of surface perpendicular to the *x,y* plane and at an angle α with the coordinate axis depend on this angle. A plot of the local value of the shear stress versus the compression stress gives a half-circle, called the Mohr stress circle, with diametral intersects $\sigma=\sigma_1$ ($\alpha=90°$, parallel to O σ_1) and $\sigma=\sigma_2$ ($\alpha=0°$, parallel to O σ_2) with the σ-axis [7]. The shear stress is maximum for $\alpha=45°$, with $\sigma=(\sigma_1+\sigma_2)/2$ and $\tau=(\sigma_1-\sigma_2)/2$ (see Fig. 4). The failure angle α between the shear plane and the direction of the major principal stress, σ_1, is $\alpha=\pi/4+\phi_e/2$, as shown in Fig. 4.

During the flow of the volume element, the local density of the solid is changing due to the consolidating influence of the compression pressures. The local

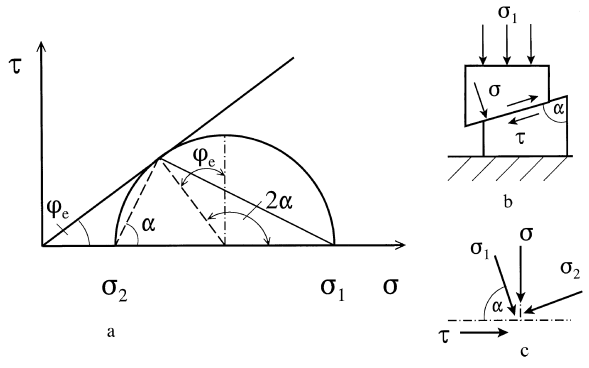

Fig. 4. Illustration of the effective yield locus; (a) the Mohr circle, the EYL, and the direction of failure of the material considered; (b) the compressed cylinder obtained in the uniaxial compression test (Fig. 5), fractured by application of a sufficiently high stress; (c) distribution of the stress directions in this experiment.

stresses, σ_i, increase in all directions. However, as we have said earlier, the ratio σ_1/σ_2 remains practically constant. A plot of the shearing stress, τ, versus the local pressure, σ, is called the yield locus, YL (Fig. 3). In discussing the onset of the flow of granular material, we must consider the influence of stress on its strength or cohesion. As long as it is unconsolidated, the material has no strength. A spoonful of packing material falls on the table as a conical heap of powder with a small (but definitively not zero) angle of repose. Such a material reacts to stress much as a liquid, however. It breaks apart under negative compression stress and shear stress is zero everywhere. When the stress increases, e.g., when the compression pressure of the solid in an axial compression column is increased, the material acquires some strength. This means that, to some extent, it can react to a negative compression stress (i.e., to a tensile stress) without breaking and while keeping its shape (not considered here) and that some shear stress exists inside the material. Not all solids behave in the same way. The tensile strength of those derived from dry, hard, and very fine materials (those we are interested in here) exhibits little increase compared to that of those typically encountered in soil mechanics (which contain fine clay particles, flat and easily deformed) and little shear stress is observed in them. Fig. 3 illustrates the definitions of the cohesion and the tensile strength.

To cause granulated solids to flow, the applied shear stress must exceed their angle of internal friction φ_i. If the point representing the stress and the pressure applied to a volume element of a free-flowing material (no cohesion) is below the effective yield locus[3] (Figs. 3 and 4), the volume does not move, the bed does not flow, and its behavior is elastic or rigid [3]. If this point is on the EYL, slip or yield takes place (in principle at an infinitely slow rate if the point is on the EYL). Note that the point cannot be above the EYL, a stress cannot exceed the flow limit. This situation of free-flowing solids is some times assumed, in soil mechanics, to be that of fine, smooth, dry sands. We know, however, that the cohesion of chromatographic packing materials is not entirely negligible under the experimental conditions of HPLC [14–16]. This is explained by the high stress applied during the packing of column beds, a stress much higher than those typical of soil mechanics.

To quantitatively describe the flow behavior of a granulated solid, the values of the characteristic parameters can be determined following the principle of the uniaxial compression test [2,3,12]. Assume a vertical, cylindrical box (Fig. 5) with a cover able to slide inside the cylinder. The box is filled with the granulated material which is, then, consolidated by compression of the top cover under a known stress, σ_1. The compression stress is removed and the hollow cylinder taken away. If the stress was sufficient, the consolidated sample keeps its cylindrical shape. If loaded, it crumbles at a stress σ_c, called the

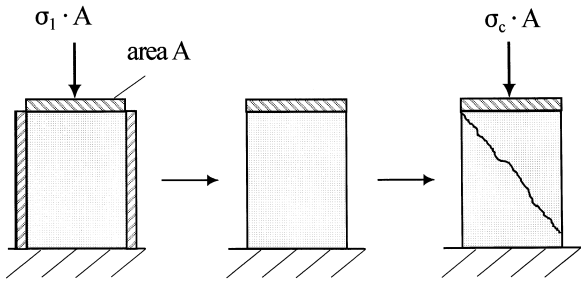

Fig. 5. Uniaxial compression test [12]. (left) Preconsolidation of a sample of the granulated material; (middle) sample ready for test; (right) fracture of the sample under uniaxial compression stress.

[3]The effective yield locus or EYL is the tangent from the origin to the Mohr stress circle corresponding to the largest compression stress applied to the material.

unconfined yield strength. A Mohr stress circle can be drawn for the sample (Fig. 3). The principal stresses are the vertical and horizontal stresses, because there is no wall friction, hence no shear against the wall. In the second part of the experiment (crushing of the consolidated sample without wall), the horizontal stress is 0 and the Mohr circle is tangent to the shear stress axis (Fig. 3). If the experiment is repeated with higher and higher consolidation stresses, a series of Mohr circles, all tangent to the vertical axis, with increasing diameters is obtained. These circles have an envelope called the yield locus (YL). It can be shown that, if samples consolidated under the same compression stress were to be crushed while a horizontal stress is also applied to them, the Mohr circle obtained, although not tangent to the vertical axis, would still be tangent to the YL. Finally, it should be noted that the YL has an end point, *E*, characterizing steady state flow.

The relationship between the unconfined yield strength and the compression stress, $\sigma_c = f(\sigma_1)$, is called the flow function of the granulated material. Because this curve is usually nearly linear, the material is often characterized by the ratio $ff_c = \sigma_1 / \sigma_c$. The larger ff_c, the more easily the solid flows (Table 1). For a given material, ff_c typically decreases with decreasing particle diameter. The relationship between the apparent bulk density and the compression stress is another important characteristic of the material. The bulk density increases with increasing compression stress. Thus, the solid flowability decreases.

The experiment just described is not a convenient method of measurement of the flow function. The lateral surface of the cylinder is not free of friction, hence of shear, and the values of the unconfined yield strength obtained by this direct method are too low. The measurements of soil cohesion are usually carried out with the JSC. This cell and the experimental procedure are described in detail in Section 3. It is sufficient to mention here that, after consolidation of the bulk material, the shear stress causing steady state flow is measured under different normal loads. The couples (σ_N, τ) determine a series of points of the YL (Fig. 3). The YL is nearly a straight line and is usually linearized. The slope of YL is the tangent of the angle of internal friction, tg φ_i ($\varphi_i < \varphi_e$) and the ordinate is the cohesion τ_c. It should be emphasized at this stage that, during any series of measurements made with the JSC to determine a YL, the density of the consolidated solid must remain constant. There is a different YL for each different value of the apparent density of the sample, i.e., for each degree of consolidation. The end points of these different YLs are on a line, the EYL. Thus, the sample must first be consolidated under a stress higher than the values of this stress under which measurements of the shear stress are carried out.

Table 1
Classification of the flow ability of bulk granulated materials

$10 < ff_c$	Free flowing
$4 < ff_c < 10$	Easy flowing
$2 < ff_c < 4$	Cohesive
$1 < ff_c < 2$	Very cohesive
$ff_c < 1$	Hard

The uniaxial compressive strength is given by [5,6]

$$\sigma_c = 2\tau_c \frac{1 + \sin\varphi_i}{\cos\varphi_i} \tag{2}$$

The normal stress, corresponding to the point of contact between the YL and the Mohr stress semicircle is [5,6]

$$\sigma_{Ta} = \tau_c \cos\varphi_i \tag{3}$$

The measurement procedure is valid if the data points used to derive the yield locus have been obtained for values of the compression stress higher than σ_{Ta}. Otherwise, the yield locus has to be recalculated, performing measurements with higher stresses. Since measurements must be carried out for compression stress between σ_{Ta} and σ_E, both unknown at the beginning, the experimental procedure involves a series of trial and error steps.

The major principal stress is given by

$$\sigma_1 = \frac{\sigma_{Pre} + \tau_c \cos\varphi_i - \sqrt{(\tau_{Pre}\sin\varphi_i + \tau_c\cos\varphi_i)^2 - \tau_{Pre}^2\cos^2\varphi_i}}{1 - \sin\varphi_i} \tag{4}$$

Finally, the effective angle of internal friction is determined by following equations [5,6]:

$$\varphi_e = \arcsin\frac{(\sigma_1 + \sigma_{Pre})^2 + \tau_{Pre}^2}{\sigma_1^2 - \sigma_{Pre}^2 - \tau_{Pre}^2} \quad (5a)$$

or

$$\varphi_e = \arcsin\frac{\sigma_1 \sin\varphi_i + \tau_c \cos\varphi_i}{\sigma_1 - \tau_c \cos\varphi_i} \quad (5b)$$

where σ_{Pre} and τ_{Pre} are the maximum normal load and shear stress, respectively.

3. Experimental

3.1. Packing materials

Two different packing materials, Kromasil NP10 (Eka Nobel, Bohus, Sweden) and Pro 10 Sil (DuPont, Karlsruhe, Germany), were used in the experiments reported here. Both materials were provided by Schering (Berlin, Germany). They had been previously used in different applications of the industrial chromatography separation process prior to their testing in our work. The nominal average particle size of the two materials was 10 μm. Both materials were first used nearly dry. Then, they were partially hydrated by exposure to the air of the laboratory. The moisture content was measured using an infra-red moisture gauge MA30 (Sartorius, Germany), based on the differential weighing of a sample before and after drying at 130°C.

To confirm this property and to determine the possible degree of particle breakage experienced by the packing materials during their previous history, the particle size distributions of these materials were measured with a laser granulometer (Sympatec Helos). The principle of particle size determination with this instrument consists in collecting the amount of light diffracted from a laser beam by a suspension of the particles flowing through a cell placed across the beam. The results of these measurements of the particle size distributions were compared with data obtained by electron microscopy (see Section 4).

Some relevant physical parameters of the two samples were also determined (see Table 2). The solid density, ρ_s, of the packing materials was measured with a helium pycnometer from Micromeritics (Northcross, GA, USA). This instrument measures the density of the skeleton of the porous particles [17]. The specific surface areas of the two materials were measured using a BET-analyzer (Areameter II from Ströhlein, Germany) and a Blaine Permeameter (Topas, Germany). The BET nitrogen gas adsorption method measures the amount of this gas adsorbed on the packing material, at equilibrium under atmospheric pressure, at the boiling point of nitrogen. This method is exact but time consuming and expensive. The Blaine permeameter measures the air flow-rate and the pressure drop through a packed bed under normalized conditions. A semi-empirical correlation gives an estimate of the surface area of contact between the bed and the air stream. The latter instrument measures the external surface area of the particles while the former measures the total surface area. For porous particles, the BET area is much larger than the Blaine area (see Table 2).

3.2. Jenike shear cell

The JSC permits the measurement of the internal friction in a granulated material, at different levels of mechanical stress, by measuring the shear stress needed to move two surfaces made of that material, one with respect to the other, as a function of the load applied between the two surfaces and of the degree of consolidation or the bulk density of the packed material.

A schematic of the JSC, shown in Fig. 6, depicts a translation shear cell, made of two half-cells, one mobile, the other immobile. The bottom half-cell is a 9.5 cm I.D., 1.4 cm deep dish, fixed to the base of the instrument. The top half-cell is a cylindrical ring

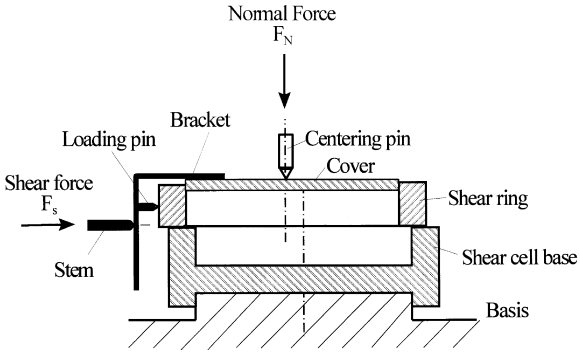

Fig. 6. Schematics of the Jenike translation shear cell [4].

of the same diameter, 1.6 cm high, closed with a cover which slides smoothly into the ring, with a narrow gap. Both half-cells are filled with the packing material. A set, vertical force, F_N, is applied to the cover of the top half-cell, with the help of a centering pin. Thus, the stress applied by the content of the top half-cell onto the content of the bottom one is born by the packing material, not by the casings. This stress is uniformly distributed over the entire surface of granulated material. Because the top half-cell is shallow, much wider than high, the load conveyed to the wall is negligible and the compression stress at the border between the two half-cells is equal to $\sigma_N = F_N/S$ (with S, surface area of the shear cell, i.e., 70.9 cm^2). A horizontal shear force is applied to the side of the top half-cell to move it by respect to the bottom half-cell. The compression and the shear stresses applied during a measurement are measured electrically, recorded and loaded in a suitable computer program which analyzes the data, using Eqs. (1)–(4), (5a), (5b).

With the JSC, it is possible to measure the effective angle of friction, φ_e, the flow function ff_c, the bulk density, and the static angle of internal friction φ_t. The shear cell measures a series of individual shear strength points $\tau = f(\sigma)$. Each set of data points gives a yield locus. The YL so obtained depends on the particle size distribution of the material studied, on the moisture content of the sample, on the temperature, and on the degree of consolidation applied prior to the measurement. Before measurements can be carried out with the JSC, the bulk density of the material must be determined because the normal loads applied depend on this density.

Measurements with the JSC must be carried out rapidly and care must be taken to avoid errors due to changes in the flow behavior of the sample of the material studied arising from an increasing moisture content (hygroscopic materials), a hardening of the material due to its drying, a strong plastic behavior of the material, chemical reactions of the material with the solvent, particle fusion or sintering under load. Difficulties are often encountered with materials having a particle diameter smaller than 4 mm.

3.3. Procedures

At the beginning of the test, before any measurement can be carried out, the material studied has to be preconsolidated in the JSC, under well-defined conditions of shear and compression stress. For this purpose, a top is placed over the sample and a force F_N is applied, causing a compression stress σ_{pre}. This stress is chosen to be the highest stress applied to the material under the standard conditions of its use. A number of oscillating twists are then applied to the cell cover to shorten the preconsolidation procedure. When preconsolidation has taken place, the normal force is removed, the loading head (connected to the shear force applicator and containing the loading pin, Fig. 6) is placed on top of the shear cell and the normal load is reapplied. The shear pin is moved at a defined velocity, applying a shear force F_S to the top-half-cell and the shear stress–strain diagram is recorded. The variation of the shear stress during the time needed to move the pin over a standard distance (6 mm) is also recorded. This later plot indicates if the material was properly preconsolidated. If not, e.g., because of an irregular preconsolidation, the previous steps must be repeated. If it has, a point of the yield locus (τ_{pre}, σ_{pre}) is derived from the steady value of the shear stress reached.

The shear pin is then moved back, the normal load is reduced ($\sigma_N < \sigma_{pre}$), and the sample is sheared again. The sample begins to flow or yield for a value, τ, of the shear stress which remains constant or decreases slightly while the sample flows, i.e., while the top half-cell slides over the bottom one. The couple (σ_N,τ) gives a point of the YL. A new sample is preconsolidated, as described above, and the process is repeated, successively to determine each point of the yield locus needed. The values of the compression stress are plotted versus those of the shear stress, giving the YL. The results of a test are valid if the bulk density has not significantly changed.

4. Results and discussion

4.1. Particle size distributions

The particle size distribution is an important factor in controlling the mechanical properties of a bulk sample of a granulated material. The coarse particles tend to move passively while the finer fraction of the

distribution carries the shear stress. Best results are obtained with a homogeneous size distribution.

The differential and cumulative particle size distributions of the two materials are reported in Figs. 7 and 8, respectively. The graphs for the two materials used are bimodal. They have a first peak at approximately 10 μm and a second maximum in the lower range of the distribution, around 4 μm. The effect is especially important in the case of Pro Sil for which the lower particle size mode is more important than for Kromasil NP 10 and is well resolved from the higher-size mode (Fig. 7). Correspondingly, the cumulative particle size distribution of Pro Sil has two steps while that of Kromasil has only a bump at its base (Fig. 8). The centers of the high size modes of the size distributions of the two samples (Fig. 7) agree with the average sizes of the particles seen in the corresponding photographs obtained with a scanning electron microscope (SEM), Fig. 9a and Fig. 10a, respectively. These SEM photographs are consistent with similar figures previously published for materials of the same origin [17]. The smallest spheres seen in Fig. 9a have a diameter of about 5–6 μm. Smaller spheres, with diameters down to ~3 μm, are visible in Fig. 10a, as parts of aggregates. Small aggregates are also seen in Fig. 10b. The presence of the finer particles (which account for a very small volume fraction of the samples) could not be ascertained by SEM and their actual existence remains in doubt. In summary, the high size modes of the particle size determinations are fully consistent

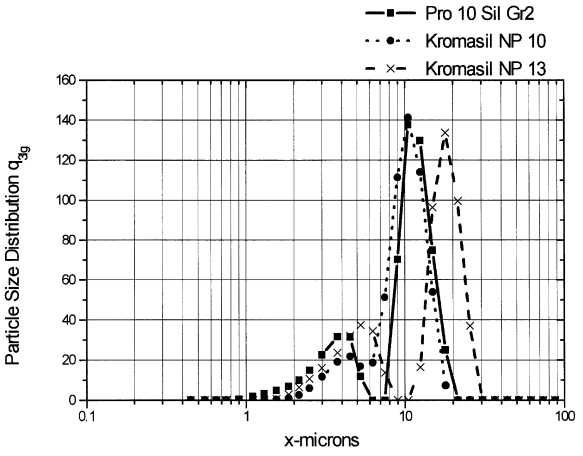

Fig. 7. Particle size distribution $q_{3,lg}$, measured with laser scattering.

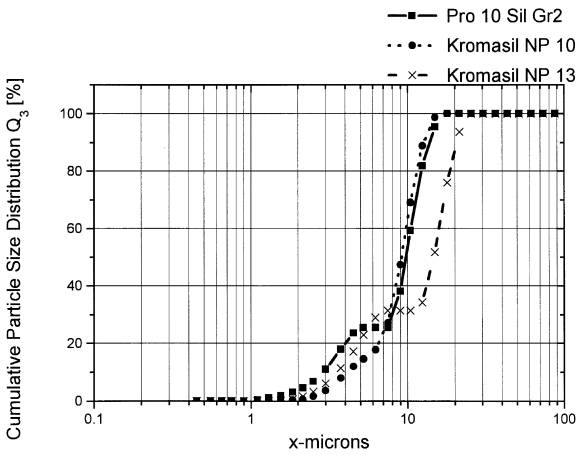

Fig. 8. Cumulative particle size distribution Q_3, measured with laser scattering.

with the SEM results and with the manufacturers' data.

It should be emphasized that there are certainly no very fine particles in the samples. This fact, together with the size distribution of a third packing material, virgin Kromasil RP8 (~13 μm in diameter), demonstrates that there was no significant amount of particle breakage during the handling of the two materials studied prior to the measurements reported here. This result is in agreement with previous data [14,15]. There is little particle breakage associated with the axial compression of spherical particles such as Kromasil [15]. If consolidation is carried out under extremely high axial compression stress (i.e., 100 bar for chromatographic packing material), a small amount of particle aggregation can also be observed [15], which does not seem to be the case in the data shown in Figs. 9 and 10. The agglomerates seen in the SEM photographs of the material (Fig. 10a and b) are the result of the preparation process of the packing material, not of previous consolidations, as shown by similar results in [14,15]. Silica beads grow from germs and, under certain conditions, larger particles can grow and engulf smaller ones, or particles of comparable size can merge. Furthermore, the particle size distribution of Kromasil RP8 is similar to that of Pro Sil (Figs. 7 and 8) which confirms that the fine particles corresponding to the low mode of the distributions do not originate from particle breakage during the axial compression of these materials prior to the present investigation.

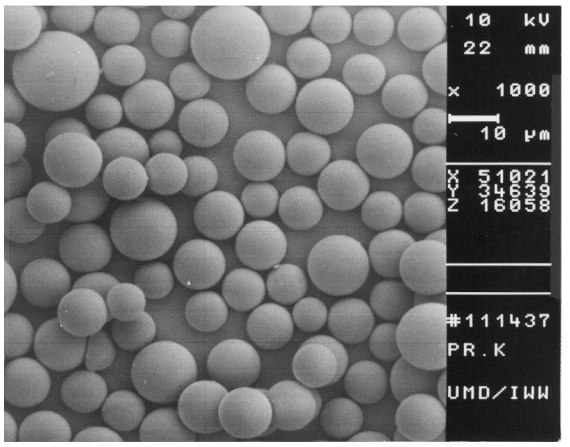

(a)

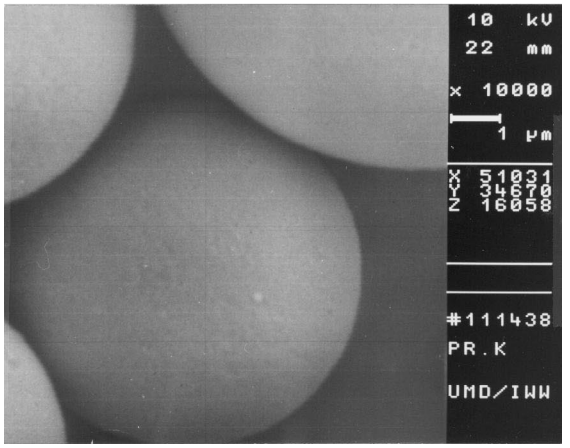

(b)

Fig. 9. Electron microscopic photography of the Kromasil NP10 sample used; (a) scale, 10 μm/cm; (b) scale, 1 μm/cm.

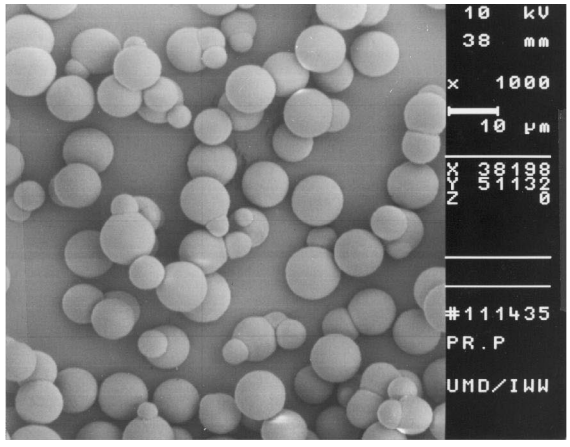

(a)

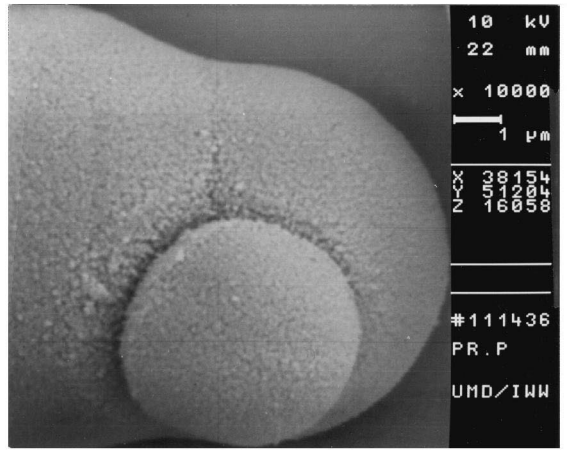

(b)

Fig. 10. Electron microscopic photography of the Pro 10 Sil sample used; (a) scale, 10 μm/cm; (b) scale, 1 μm/cm.

The values measured for the other relevant parameters are shown in Table 2. The bulk density of the porous particles suggests that there are slightly more closed pores in the Kromasil sample than in the somewhat denser Pro Sil. The specific surface areas of the two materials measured by BET with nitrogen ($A_{m,BET}$) show that Kromasil has nearly twice the specific surface area of Pro Sil. The Sauter diameters (Table 2) are parameters often used in the study of granulated materials. They are the diameters of hypothetical monosized, spherical solid particles having the same specific surface area as the material under study. They were derived from the particle size distributions, from the BET data and from the Blaine data. The BET value ($d_{ST,BET}=6/(A_{m,BET}\cdot\rho_s)$) is indicative of the average size of the primary particles, the coalescence of which leads to the porous silica particles. Values of 8 and 15 nm were obtained for Kromasil and Pro Sil, respectively.

The Blaine permeameter measures a property which is quite different from the specific surface areas determined by nitrogen-BET. The BET surface area is the surface area of the pores inside the silica particles. The Blaine area is derived from gas permeability data and is calculated with a modified Carman–Kozeny equation [13]. Thus, it is related to

Table 2
Granulometric parameters of packing material

No.	Parameter	Kromasil NP 10	Pro 10 Sil Gr 2
1	Mean particle diameter, $d_{50,3}$ (μm)	9.2	9.9
2	Sauter diameter, d_{ST} (μm) (calculated from the particle size distribution)	7.4	6.2
3	Solid material density, ρ_B (g/cm^3)	2.239	2.324
4	Blaine surface area, $A_{m,BL}$ (m^2/g) (permeameter)	1.5	1.1
5	Sauter diameter, d_{ST} (μm) (calculated from the Blaine surface)	1.8	2.3
6	BET surface, $A_{m,BET}$ (m^2/g) (N_2-adsorption, areameter II)	318	175
7	Sauter diameter, d_{ST} (nm) (calculated from the BET surface)	8	15

the external surface area of the particles. The difference between the two values is in agreement with those generally observed with powders [18]. The results of the Blaine test suggest that the particle size distribution, the particle shape, and the surface roughness of the particles influence the permeability of the bulk material. Although both materials have approximately the same mean particle diameter, Kromasil, which has more regular shaped particles with a lesser amount of fine ones has a slightly larger Blaine surface area than Pro Sil, a result not entirely consistent with the other observations.

4.2. Results of the shear stress study

The materials were initially nearly dry when used. It was observed that they flowed like liquids, a behavior which was attributed to their pores not being saturated with a liquid, by analogy with similar observations frequently made with fine sands. Under such conditions, it was very difficult to consolidate the materials under axial stress in the shear cell. Therefore, the use of a solvent was deemed necessary and water, which wets well the unbonded silica used here, was selected. The tests were performed with two different moisture contents. First, the moisture contents of Kromasil and Pro Sil were adjusted to 5.3 and 1.6%, respectively by a short-term exposure to the laboratory atmosphere. Then, the moisture content was increased with addition of water to nearly saturated conditions. The corresponding water contents were 79 and 67%, respectively. The results of the shear stress tests obtained with these wet materials are summarized in Table 3 and Figs. 11 and 12. The graphical displays in these figures show the $\sigma-\tau$-diagrams with the different Mohr stress semi-circles (dotted and dashed lines). The symbols represent the data points recorded. The

Table 3
Results of the tests carried out with the Jenike shear cell

	Kromasil NP 10		Pro 10 Sil	
	Dry	Saturated	Dry	Saturated
$X_l = m_l/m_s \times 100$ (%)	5.3	79	1.6	67
σ_{pre} (kPa)	3.9	4	3.9	4.0
σ_1 (kPa)	6.6	6.1	6.4	8.1
σ_c (kPa)	[a]	0.8	[a]	1.1
ff_c (−)	∞	8	∞	6.5
φ_i (°)	24	23	30	36
φ_e (°)	24	26	30	40
ρ_b (g/cm^3)	0.531	0.772	0.529	0.849

[a] Below the detection limit, i.e., practically 0.

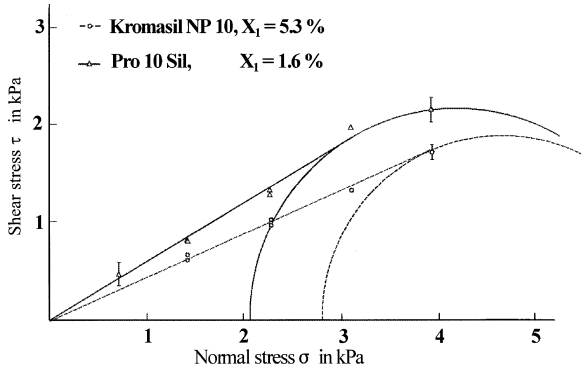

Fig. 11. Yield locus of Kromasil NP10 and Pro 10 Sil under initial conditions.

straight lines derived from these data are the corresponding yield loci. These results allow a detailed description of the solid-flow properties of the particles of the packing material.

The data in Table 3 show that the angles of internal friction, ϕ_i and ϕ_e, are smaller for Kromasil than for Pro Sil. This means that there is less internal friction in a column packed with Kromasil than in one packed with Pro Sil. This conclusion is also supported by the smaller values of the uniaxial compression strength, σ_C, and the cohesion strength, τ_C. An increase of the internal friction hinders the flow behavior. The differences observed in the flow behavior of the two materials could be explained by a combination of these following properties:

(1) Stable agglomerates are seen in Fig. 10a and not in Fig. 9a. These agglomerates are not spherical

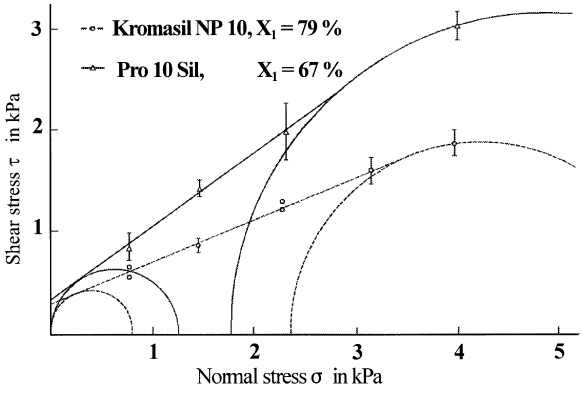

Fig. 12. Yield locus of Kromasil NP10 and Pro 10 Sil under saturated conditions.

and this may obstruct the flow and increase the angle of internal friction. The presence of these agglomerates causes a decrease of the external porosity of Pro Sil.

(2) The particles of Pro Sil are rougher than those of Kromasil (cf. Fig. 9b and Fig. 10b). The friction at their contact is higher.

Finally, the difference of the solid-flow behaviors of Kromasil and Pro Sil is also confirmed by the values of their flow functions, ff_c (Table 3), which are 8 and 6.5, respectively. Although these values place both materials in the easy flowing group, they are sufficiently different to signal a marked difference in flow behavior of the two packing materials. The ratio σ_1/σ_c is supposed to remain constant for a given material, consolidated under a certain compression load. As shown in Table 3, both materials flow easily but Kromasil has the higher value, and so flows more freely than Pro Sil. Note the large influence of the water content on these data, particularly σ_c.

5. Conclusion

The flow behavior of fine disperse materials is determined by surface properties of their particles and by phenomena involving interparticular interactions. Due to these complex interactions, the observed effect cannot be described simply in these preliminary tests. The most important limits to the applicability of our results to a discussion on the packing of chromatographic columns arise from the facts that the performed tests were carried out (1) under preconsolidation stresses which were several orders of magnitude lower than those encountered in chromatographic columns and (2) using particles which were wet with water, not immersed in a conventional packing solvent. These differences were caused by the necessity to use the available instrumentation, designed for the study of the typical granulated materials encountered in soil mechanics, under the kind of stress used in civil engineering.

Still, the tests performed with the JSC show a significantly different behavior of the two packing materials. The angle of internal friction for Kromasil is smaller than that of Pro Sil, especially under saturated conditions. When the water content of the

particles increased, the angle of internal friction of Kromasil remained nearly constant (Table 3). That of Pro Sil increased. Thus, the particles of Pro Sil stick tighter together and do not flow as easily as those of Kromasil.

These differences show that the flow properties of granulated materials, still ignored in chromatography, may be quite important, that they can be measured precisely, and can be characterized by parameters which are well established in other fields of science. Accordingly, investigations should be pursued along this line. Measurements of the flow properties of a large number of virgin samples of different packing materials should be carried out. The experimental conditions must be adjusted, using a higher degree of liquid saturation, different liquids, and higher values of the compression and the shear stress. A study of the influence of the specific surface area of the packing material and of its porosity on its flow properties might also prove useful. Further experiments are in process. Their results should lead to a better understanding of the behavior of packing material during the packing of chromatographic columns and may help us in making better columns.

6. Symbols

$A_{m,BET}$	BET surface (m^2/g)
$A_{m,Bl}$	Blaine surface (m^2/g)
d_{St}	Sauter diameter or specific surface area (μm)
$d_{50,3}$	Mean particle diameter (μm)
ff_c	Flow function (−)
F_N	Normal load (N)
F_S	Shear load (N)
h	Height (mm)
P_h	Horizontal pressure (kPa)
P_L	Isostatic pressure of a liquid with the some packing density as it has as a powder (kPa)
P_v	Vertical pressure (kPa)
Q_3	Cumulative particle size distribution (%)
q_{3lg}	Particle size distribution
X_i	Relative moisture content (%)
x	Particle size (μm)
α	Failure angle (°)
λ	Horizontal pressure ratio
ρ_b	Bulk density (kg/m^3)
ρ_S	Solid density (kg/m^3)
ϕ_c	Effective angle of friction (°)
ϕ_i	Static angle of internal friction (°)
σ_2	Compression stress (kPa)
σ_1	Major pressure (kPa)
σ_2	Minor pressure (kPa)
σ_2	Normal stress (kPa)
σ_{pre}	Specific normal stress by preconsolidation (kPa)
σ_c	Unconfined yield strength (kPa)
σ_T	Tensile strength (kPa)
σ_{Ta}	Normal stress at the point where YL is tangent of Mohr's circle (kPa)
τ_{pre}	Preshear stress (kPa)
τ_c	Cohesion (kPa)
τ_W	Wall shear stress (kPa)

Acknowledgements

This work has been supported in part by the Grant DE-FG05-88ER13859 of the US Department of Energy and by the cooperative agreement between the University of Tennessee and the Oak Ridge National Laboratory. We thank G. Mann (Schering, Berlin, Germany) for the gift of large amounts of stationary phase, U. Wendt and H. Heyse (Department of Material Sciences, Magdeburg Universität) for the SEM photographies and A. Al-Hilo for his contribution to the measurements.

References

[1] H.M. Jaeger, S.R. Nagel, R.P. Behringer, Rev. Modern Phys. 68 (1996) 1259.
[2] J.-P. Bardet, Experimental Soil Mechanics, Prentice Hall, Upper Saddle River, NJ, 1997.
[3] J. Schwedes, D. Schultze, Powder Technol. 61 (1990) 59.
[4] A.W. Jenike, Storage and Flow of Solids: Bulletin No. 123, University of Utah, Utah Engineering station, Vol. 23, No. 26, 1964.
[5] J. Tomas, Zum Verfestigungsprozess von Schuettguetern, Mikroprocesse und Kinetikmodelle, CIT 69 4, 1997, pp. 455–467.
[6] J. Tomas, Modeling Time Consolidation Processes of Bulk Materials — Problems and Preliminary Solutions, in: G.G. Enstad, Proc. 2nd Int. Symp. on Reliable Flow of Particulate Solids, Aug. 1993, Oslo, Porsgrunn, Norway, pp. 342–379.

[7] A.R. Jumikis, Theoretical Soil Mechanics, van Nostrand, New York, NY, 1969.
[8] A.D. Visser, Elseviers Dictionary of Soil Mechanics (in four languages), Elsevier, Amsterdam, 1965.
[9] T.W. Lambe, R.V. Whitman, Soil Mechanics. SI Version, Wiley, New York, 1979.
[10] J. Schwedes, Ph.D. Dissertation, University of Karlsruhe, Karlsruhe, 1971.
[11] O. Molerus, Schüttgutmechanik, Grundlagen und Anwendungen in der Verfahrenstechnik, Springer Verlag, Berlin, 1985.
[12] D. Schulze, Measuring Powder Flowability: A Comparison of Test Methods, Part I, in Powder and Bulk Engineering, April 1996.
[13] J.M. Coulson, J.F. Richardson, Chemical Engineering: Particle Technology and Separation Processes: Vol. 2, Pergamon Press, Elmsford, NY, 4th ed., 1990.
[14] M. Sarker, G. Guiochon, J. Chromatogr. A 702 (1995) 27.
[15] M. Sarker, A.M. Katti, G. Guiochon, J. Chromatogr. A 719 (1996) 275.
[16] T. Yun, G. Guiochon, J. Chromatogr. A 760 (1997) 17.
[17] H. Guan, G. Guiochon, D. Coffey, E. Davis, K. Gulakowski, D.W. Smith, J. Chromatogr. A 736 (1996) 21.
[18] S. Lowell, Introduction to Powder Surface Area: John Wiley, New York, 1979